Jet Penetration Height in Transonic Flow

Jonah Manela*
Armaments Development Authority, Haifa, Israel
and
Arnan Seginer†
Technion—Israel Institute of Technology, Haifa, Israel

A penetration height of a circular underexpanded transverse jet into a uniform transonic flow is formulated. It is an extension of Spaid's jet penetration height in supersonic flow and is based on a momentum balance in the expanding and bending jet. The newly defined penetration height is used to correlate pressure data from several experiments with different test conditions. The effects of an axisymmetrical jet emission from a cylindrical body on its aerodynamic characteristics is approximated by the addition to the cylinder of an equivalent flare.

Nomenclature

A = throat cross-sectional area of injection nozzles, Eq. (12)
C_D = drag coefficient, D/qS
C_j = nozzle discharge coefficient, $\dot{m}_j/\rho_j V_j A_j$
C_N = normal force coefficient, N/qS
C_p = pressure coefficient, $(p-p_\infty)/q$
d = nozzle diameter
D = body diameter, also drag
h = jet penetration height
M = Mach number
$\dot{m}$ = mass flux
N = normal force
n = number of jets
p = pressure
q = freestream dynamic pressure, $\frac{1}{2}\rho_\infty V_\infty^2$
R = gas constant
S = model cross-sectional area
T = temperature
V = velocity
X = streamwise distance measured upstream from the jets
α = angle of attack
γ = specific heat ratio
ϕ = circumferential angle
ρ = density

Subscripts

CP = center of pressure
j = jet parameters
t = nozzle throat parameters
∞ = freestream conditions
0 = stagnation conditions

Introduction

THE interaction of a uniform flow with a transverse jet can be found in short takeoff and landing (STOL) aircraft, in thrust vector control, and in direct vehicle attitude control. It is characterized by an effective jet thrust that is larger than the conventional thrust (obtained by blowing into a stagnant medium), as a result of the interaction of the jet with the surrounding flowfield. Early studies of this flow interaction phenomenon concentrated on the interaction of a single, usually sonic, two-dimensional jet with an external supersonic flow. Most studies were experimental because of the complexity of the problem.

The high level of complexity of this problem is demonstrated by a representative study of a two-dimensional interaction of a supersonic planar flow with a transversal sonic jet that was published by Spaid and Zukoski.[1] The typical features of the interaction flowfield and the resulting pressure distribution are shown in Fig. 1 (taken from Ref. 1). The jet acts as an obstacle to the main flow, generating a shock wave and forcing the flow to separate and lift off the surface in order to negotiate the obstacle. The separation shock generates a sharp pressure rise, followed by a pressure plateau. A bow shock that forms near the jet causes an additional pressure rise after the plateau. The jet is bent aft by the high-pressure region and a low-pressure separation region forms behind it. Farther downstream, the combined jet and outer flow reattach through a recompression shock. The flowfield described in Fig. 1 resembles a supersonic flow over a forward-facing step; thus, several investigators[2-4] have used an equivalent solid body to simulate the jet's disturbance to the main flow.

The solid-obstacle approximation can also be extended to three-dimensional interactions. The three-dimensional interaction of a circular jet with a supersonic planar flow is, in principle, similar to the two-dimensional interaction described above (Fig. 2a, taken from Ref. 5). However, extent and intensity of the three-dimensional interaction are reduced because the flow can go around the obstacle in addition to going over it (the three-dimensional relief effect[6]). The typical pressure distribution in the vicinity of a pair of jets (Fig. 2b) shows even more similarity to the two-dimensional case[5,7] and indicates that this similarity increases when the number of jets increases and their separation decreases.

While most of the research effort concentrated on supersonic interactions that were common in thrust vectoring and direct attitude control of missiles, very little work was done on transonic interactions. The scant information (e.g., Fig. 3, taken from Ref. 8) available when this work was commenced showed that the transonic interaction was, generally speaking, similar in character to the previously described supersonic one. The main differences were that the pressure gradients were weaker, the pressure plateau was very short and vanished at low blowing pressure ratios (p_{0j}/p_∞), and the shock waves were weak normal shocks.

Presented as Paper 83-1680 at the AIAA 16th Fluid and Plasma Dynamics Conference, Danvers, MA, July 12-14, 1983; received Nov. 1, 1984; revision received April 25, 1985.

*Research Scientist.
†Associate Professor, Department of Aeronautical Engineering (National Research Council Senior Research Associate at NASA Ames Research Center, California, at the time of paper presentation and submission). Member AIAA.

With the development of STOL fighter aircraft and guided and maneuvering munitions, the interest in transonic interactions increased. The authors of this paper studied the uncharted interaction of several circular supersonic jets with an external transonic flow.[9] A further difference from previous studies was that these dealt with blowing from a flat plate into a planar flow, whereas in this study a number of circular, radial jets were injected symmetrically from the perimeter of the base of an axisymmetrical body into a three-dimensional outer flow. In this case, the jets did not generate any direct net forces or moments on the body. The forces and moments that were actually measured, when the body was positioned in the flow at an angle of attack, were the result of small pressure differences between the interaction regions on the windward and leeward sides of the body. Thus, the ability to predict the effect of the interaction became even more important.

Because of the complexity of the flowfield and the difficulties in describing it theoretically, attempts were made to correlate its features with the governing parameters. One of these correlation parameters was Spaid's jet penetration height in supersonic flow.[10] Spaid's correlation method, being supersonic, could not, however, be applied to the present transonic flow. Therefore, the purpose of this work was to modify Spaid's correlation parameter and to adapt it to transonic flow.

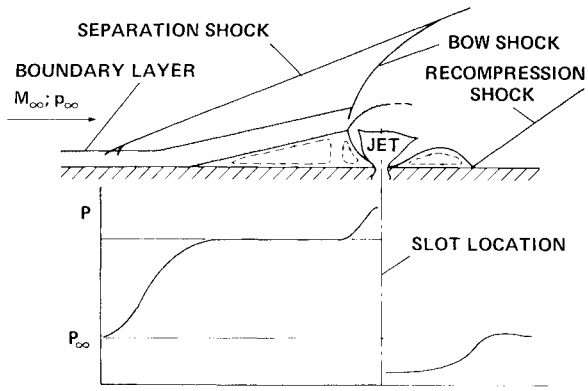

Fig. 1 Flowfield and pressure distribution of a supersonic flow over a two-dimensional jet (from Ref. 1).

A Jet Penetration Height in Supersonic Flow

Based on their experimental data, Spaid and Cassel[7] listed the parameters that governed the flowfield interaction generated by the jet penetration as: 1) the geometry of the model and blowing nozzles, 2) main flow Mach and Reynolds numbers, 3) ratio of specific heats of the injectant, 4) blowing pressure ratio (p_{0j}/p_∞), and 5) total temperature and molecular weight ratio.

However, Chrans and Collins[11] showed that as far as only the pressure interaction field is concerned, hot jets could be simulated by cold-flow experiments. They found no influence of the jet's total temperature or molecular weight on the interaction within the range of parameters investigated in Ref. 9.

Spaid[10] included these parameters (except for the Reynolds number, total temperature, and molecular weight ratio) in his formulation of a correlation parameter—the jet penetration height—by which the experimental results from different supersonic tests could be correlated. It was defined as the effective height of the external flow's disturbance caused by the jet and was analogous to the height of an equivalent solid obstacle. Spaid's formulation of the penetration height of a circular underexpanded sonic jet into a planar supersonic flow required the following assumptions:

1) The penetration height is large compared with the boundary-layer thickness of the undisturbed flow.

2) The jet expands isentropically to the ambient pressure while being bent in the direction of the free flow.

3) The jet and external flow do not mix.

4) The contact surface between the two flows is shaped like a quarter-sphere attached to half of a cylindrical afterbody.

5) The pressure distribution over the spherical contact surface is calculable by Newtonian theory.

6) The jet penetration height h is defined as the radius of the quarter-sphere contact surface and its value can be determined by a momentum balance in the flow direction. The control volume for this momentum balance is delimited by the quarter-sphere described above, the flat surface from which the jet is injected, and a plane perpendicular to the free flow that passes through the rear of the quarter-sphere.

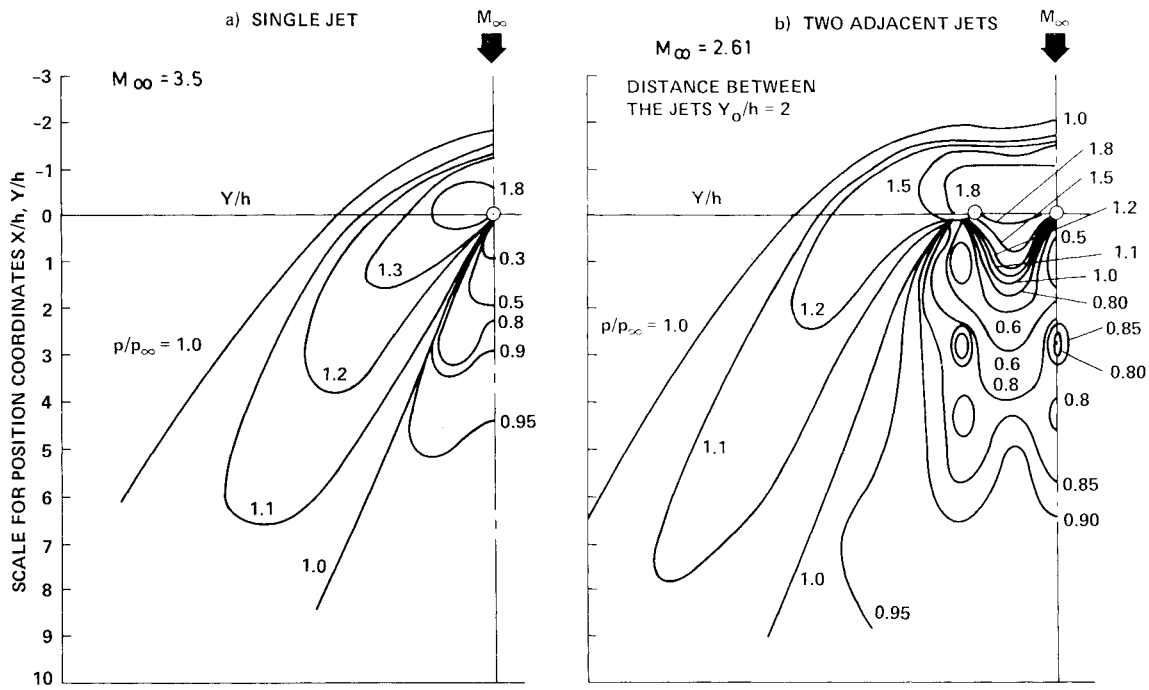

Fig. 2 Typical pressure distributions around one and two circular jets interacting with a supersonic flow (from Ref. 5).

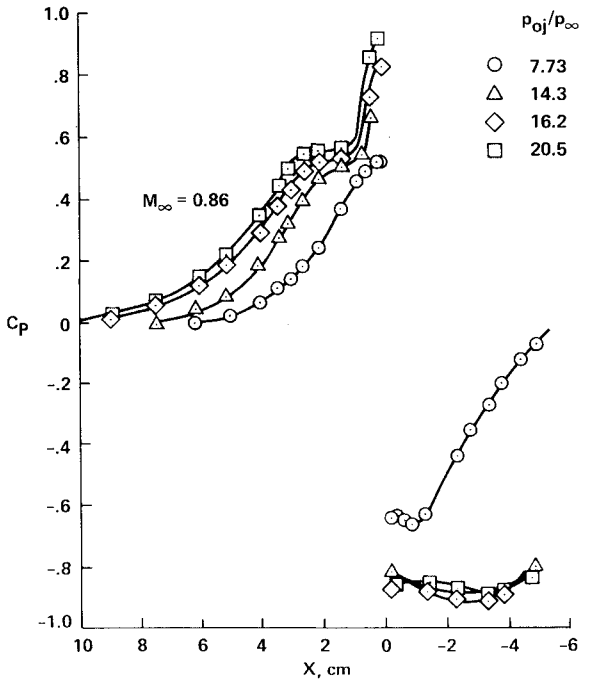

Fig. 3 Typical pressure distributions in a transonic interaction (from Ref. 8).

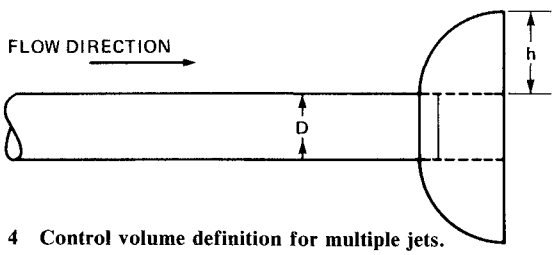

Fig. 4 Control volume definition for multiple jets.

Based on these assumptions, Spaid's momentum balance results in the penetration height given by

$$\frac{h}{d_t} = \frac{1}{M_\infty}\left(\frac{2C_j}{C_p^*}\frac{p_{0j}}{p_\infty}\right)^{1/2}\left\{\frac{2}{\gamma_j - 1}\left(\frac{2}{\gamma_j + 1}\right)^{(\gamma_j+1)/(\gamma_j-1)} \times \left[1 - \left(\frac{p_\infty}{p_{0j}}\right)^{(\gamma_j-1)/\gamma_j}\right]\right\}^{1/4} \tag{1}$$

where C_p^* is the stagnation pressure coefficient behind a normal shock wave:

$$C_p^* = \frac{2}{\gamma_\infty M_\infty^2}\left[\left(\frac{\gamma_\infty + 1}{2}M_\infty^2\right)^{\gamma_\infty/(\gamma_\infty-1)} \times \left(\frac{\gamma_\infty + 1}{2\gamma_\infty M_\infty^2 - \gamma_\infty + 1}\right)^{1/(\gamma_\infty-1)} - 1\right] \tag{2}$$

The term C_p^* was used by Spaid to calculate the drag on the quarter-sphere by the Newtonian theory. An examination of Eq. (1) results in the approximate relationship

$$h/(d_t C_j^{1/2}) \propto (1/M_\infty)(p_{0j}/p_\infty)^{1/2}$$

or, after rearranging:

$$h \propto [(d_t^2 C_j p_{0j})/(M_\infty^2 p_\infty)]^{1/2} \tag{3}$$

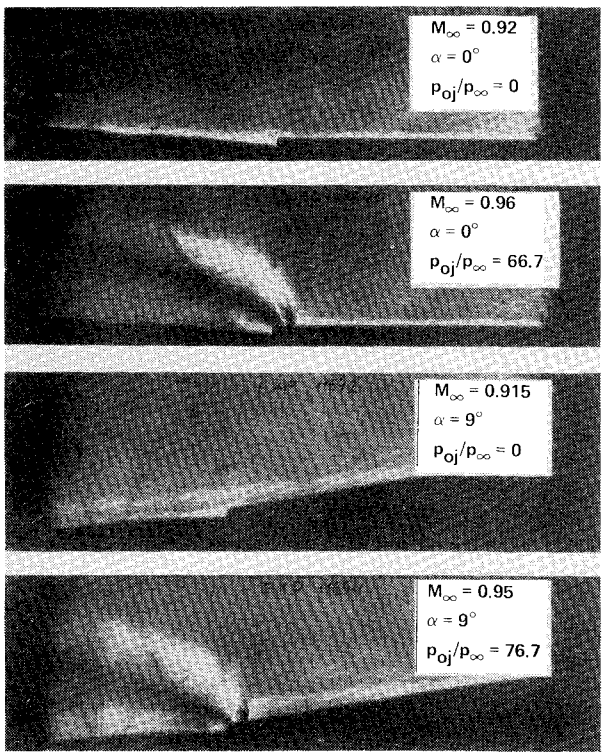

Fig. 5 Single-jet influence on the boundary layer.

which means that the penetration height is proportional to the square root of the ratio of the jet thrust to the freestream dynamic pressure. Other attempted correlations, like those of Refs. 12 and 13 based on the jet momentum flux (or thrust), also concluded that the interaction was governed by the ratio of the jet momentum to the specific momentum of the free flow.

A Jet Penetration Height in Transonic Flow

Spaid's jet penetration height h was useful for correlating the pressure distributions obtained in different tests.[10] For a similar correlation in the present work, the jet penetration height must be redefined for transonic flow. For a single jet, Spaid's assumptions and formulation can be used, except for the drag coefficient on the quarter-spherical face of the control surface. Instead of the drag being calculated by the Newtonian theory with the assumption of a strong normal bow shock upstream of the spherical surface, it is approximated in the transonic case by the empirical relation (Ref. 6, p. 410),

$$C_D \approx C_{p_{0\infty}} - 0.5 \quad (\text{for } 0.7 < M_\infty < 1.2) \tag{4}$$

where $C_{p_{0\infty}}$ is the freestream stagnation pressure coefficient. Although $C_{p_{0\infty}} = C_p^*$ for $M_\infty = 1$, they differ significantly anywhere else in the transonic range, and C_p^* is meaningless for $M_\infty < 1$. With this drag coefficient, the momentum balance results in

$$\frac{h}{d_t} = \frac{1}{M_\infty}\left(\frac{C_j}{C_{p_{0\infty}} - 0.5}\frac{\gamma_j}{\gamma_\infty}\frac{p_{0j}}{p_\infty}\right)^{1/2} \times \left\{\frac{2}{\gamma_j - 1}\left(\frac{2}{\gamma_j + 1}\right)^{(\gamma_j+1)/(\gamma_j-1)} \times \left[1 - \left(\frac{p_\infty}{p_{0j}}\right)^{(\gamma_j-1)/\gamma_j}\right]\right\}^{1/4} \tag{5}$$

The full derivation of Eq. (5) and of the following expressions is given in detail in Ref. 14. For experiments in cold flows (wind tunnel and jet flows) with $\gamma_j = \gamma_\infty = 1.4$, one derives

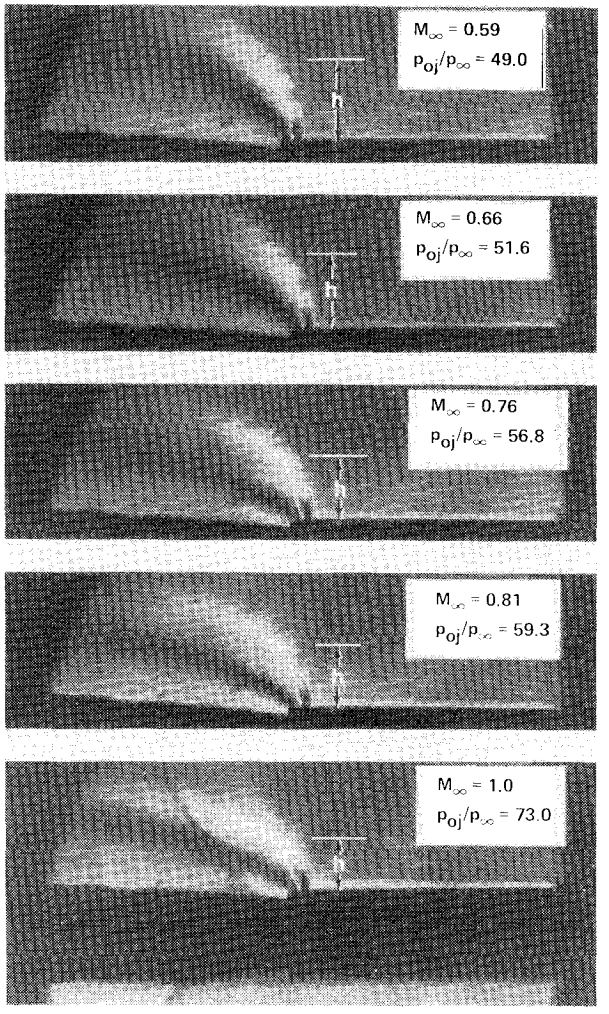

Fig. 6 Mach number and pressure ratio effects on a single-jet penetration.

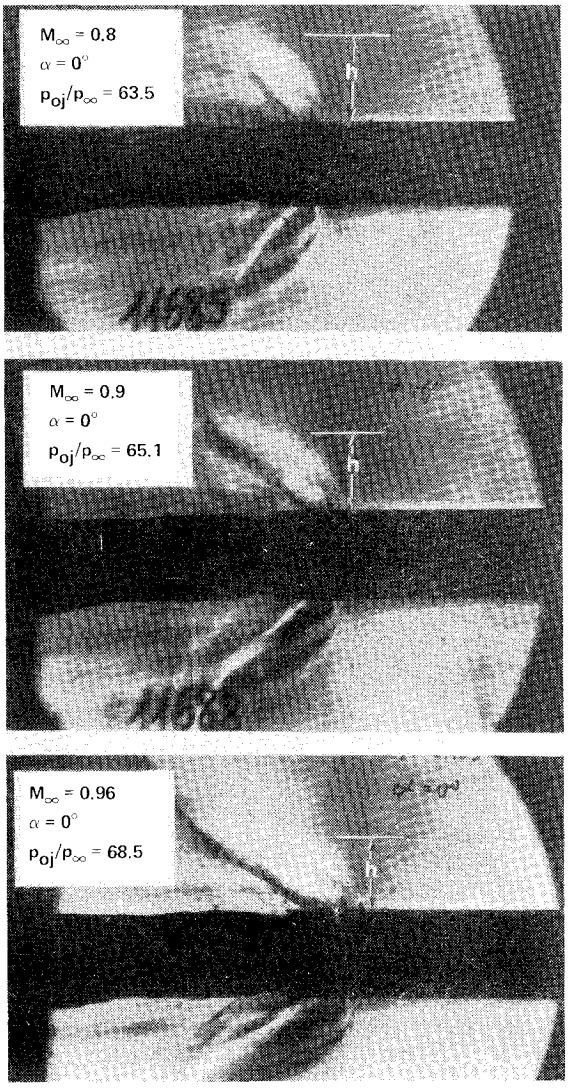

Fig. 7 Schlieren photographs of the flowfield induced by eight jets.

from Eq. (5)

$$\frac{h}{d_t(C_j)^{1/2}} = \frac{1}{M_\infty}\left(\frac{1}{C_{p_{0\infty}} - 0.5}\,\frac{p_{0j}}{p_\infty}\right)^{1/2} \times \left\{1.6745\left[1 - \left(\frac{p_\infty}{p_{0j}}\right)^{0.2857}\right]\right\}^{1/4} \tag{6}$$

This formulation was derived for a single jet injected from a flat plate into a planar transonic flow. For the case of a single jet injected from an axisymmetric body of diameter D, as was the case in the experiments of Ref. 9, Eq. (6) would be valid only if $h/D \ll 1$. It is assumed that for higher values of h/D, Eq. (6) would still correctly describe the *trends* of the penetration height with varying jet and free-flow parameters. However, the derivation of the penetration height must be modified when it is to be used to correlate the results of multiple jets injected radially from an axisymmetric body.[9]

Using Spaid's assumptions, it is also assumed that the disturbance of a number (n) of discrete circular jets can be approximated by a continuous, axisymmetric radial jet injected around the body perimeter, with a thrust that equals the combined thrust of the discrete jets. This is consistent with the observations of Refs. 5 and 7 (Fig. 2). The momentum balance in this case is calculated for an annular control volume (Fig. 4) that is bounded by 1) the toroidal contact surface between the free flow and the jet, 2) the surface of the body, and 3) a radial plane that intersects the contact surface at the point where the jet flow becomes parallel to the freestream. Referring to Fig. 4, the momentum balance is given by[14]

$$\dot{m}_j V_j = \tfrac{1}{2}(\gamma_\infty p_\infty M_\infty^2 C_D)\,(\pi/4)[(D+2h)^2 - D^2] \tag{7}$$

where $\dot{m}_j$ is the combined mass flux of n jets

$$\dot{m}_j = C_j A_j p_{0j}\left[\frac{\gamma_j}{R_j T_{0j}}\left(\frac{2}{\gamma_j+1}\right)^{(\gamma_j+1)/(\gamma_j-1)}\right]^{1/2} \tag{8}$$

$$A_j = n(\pi/4)d_i^2 \tag{9}$$

and the jet exit velocity is

$$V_j = \left\{\frac{2\gamma_j}{\gamma_j - 1} R_j T_{0j}\left[1 - \left(\frac{p_\infty}{p_{0j}}\right)^{(\gamma_j-1)/\gamma_j}\right]\right\}^{1/2} \tag{10}$$

Substituting Eqs. (8-10) in Eq. (7) and using the empirical approximation for C_D [Eq. (4)], the solution for the penetration height from Eq. (7) is

$$h^2 + Dh = \left[\frac{C_j d_i^2 n}{M_\infty^2(C_{p_{0\infty}} - 0.5)}\right]\frac{p_{0j}}{p_\infty} \times \left\{\frac{\gamma_j^2}{2(\gamma_j-1)}\left(\frac{2}{\gamma_j+1}\right)^{(\gamma_j+1)/(\gamma_j-1)} \times \left[1 - \left(\frac{p_\infty}{p_{0j}}\right)^{(\gamma_j-1)/\gamma_j}\right]\right\}^{1/2} \tag{11}$$

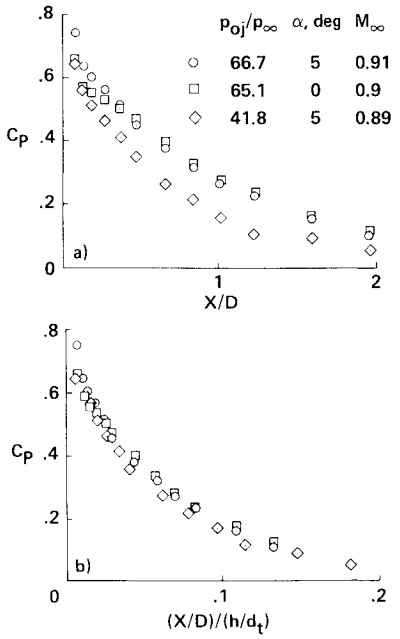

Fig. 8 Pressure distributions at $\alpha = 0$ and 5 deg: a) not normalized; b) normalized by penetration height.

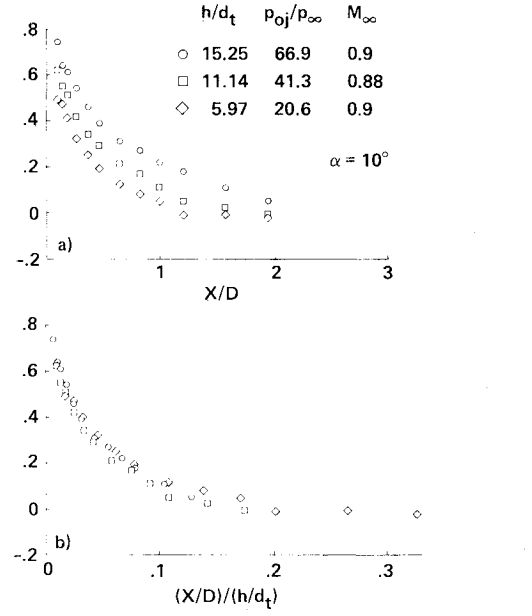

Fig. 9 Pressure distributions at $\alpha = 10$ deg: a) not normalized; b) normalized by penetration height.

The number of jets (n) must be high to justify the assumption of a continuous circumferential disturbance.

Results and Discussion

The experimental part of this investigation, described in Ref. 9, was done on an ogive cylinder model, with radial jets injected into the outer transonic flow around the perimeter of its base. The program included tests with a single radial jet and with eight jets around the model base circumference. The main test parameters were the free-flow Mach number, the model angle of attack, and the blowing pressure ratio (p_{0j}/p_∞). Schlieren photographs of the flow were taken. The pressure distribution over the last two diameters of the model was recorded and integrated to produce the lift coefficient and the location of the center of pressure.[9]

Typical schlieren photographs of the interaction of a single jet with the transonic flow are shown in Figs. 5 and 6. Figure 5 shows the effects of the jet on the boundary layer at angles of attack of 0 and 9 deg. The thickening of the boundary layer due to the jet is not large. At $\alpha = 9$ deg, the boundary layer is separated some 1.5 body diameters upstream of the base, even without the jet disturbance. Figure 5 justifies the assumption that the jet penetration height is larger than the undisturbed boundary-layer thickness.

As the freestream Mach number is increased, the jet is turned downstream closer to the body (Fig. 6), as expected, because of the increasing drag on the jet, in spite of the increasing blowing pressure ratio. With a fixed tunnel stagnation pressure, the freestream static pressure p_∞ was decreasing when the Mach number was rising. The resulting increased blowing pressure ratio tends to increase the jet's physical penetration height, but its effect is overcome by the simultaneously increasing Mach number.

Also shown in Fig. 6 is the penetration height calculated from Eq. (6). It does not correspond to any physical feature of the flowfield and should be considered only as a similarity parameter. However, a qualitative agreement between the calculated penetration height and the jet radius of curvature is observed (Fig. 6). The counteracting effects of the freestream Mach number and of the blowing pressure ratio discussed above are clearly seen in Eq. (6). The dominance of M_∞ to the first power over the square root of (p_{0j}/p_∞) agrees with the experimental results of Fig. 6.

Although the character of the eight-jet interaction, as seen in its schlieren photographs (Fig. 7), differs from that of the single-jet interaction (Fig. 6), the penetration height calculated from Eq. (11) and marked on these photographs shows again the same trend as the radius of curvature of the jets, as well as the dominant effect of the Mach number. The pressure distributions with eight active jets, presented in Refs. 9 and 14 for $\alpha = 0$ deg, indicate that the flow was nearly axisymmetric. The only deviations from an axisymmetric flow were measured very close to the origins of the jets, where high pressures were observed in line with the nozzles and lower pressures were observed between them. This is in agreement with the observations of Ref. 5 (Fig. 2) and justifies the present approximation of the discrete jets by an equivalent axisymmetric obstacle [Eqs. (7-9)].

The pressure distributions reported in Refs. 9 and 14 were found to be strongly dependent on the blowing pressure ratio. It is shown in Fig. 8a that the blowing-pressure effect is much stronger than the influence of an angle-of-attack change from 0 to 5 deg. Figure 8b proves that these effects can be correlated with the penetration height as given by Eq. (11); the data nearly collapse on a single curve. Although the derivation of the penetration height is valid only for $\alpha = 0$ deg, the $\alpha = 5$ deg data also correlate fairly well. Figure 9a shows the blowing-pressure effect at an angle of attack of $\alpha = 10$ deg and, again, these data are correlated by the computed penetration height in spite of the relatively large angle of attack.

The Equivalent Flare

The interaction between a transonic flow and transverse supersonic jets has never been solved numerically and such a computation, although probably possible, would not be cost effective. However, the aforementioned concept of an equivalent solid obstacle gives rise to the following crude approximation that can be used for engineering design purposes. Both the schlieren pictures (Fig. 7) and the pressure distributions (Figs. 8 and 9) of the eight-jet induced flowfield resemble those obtained on flared-cylinder models. Although the obstacle presented to the flow by the jets is not conical, the rapid thickening of the boundary layer because of the adverse pressure gradient, is roughly conical. Boundary-layer measurements from the schlieren pictures defined a conical

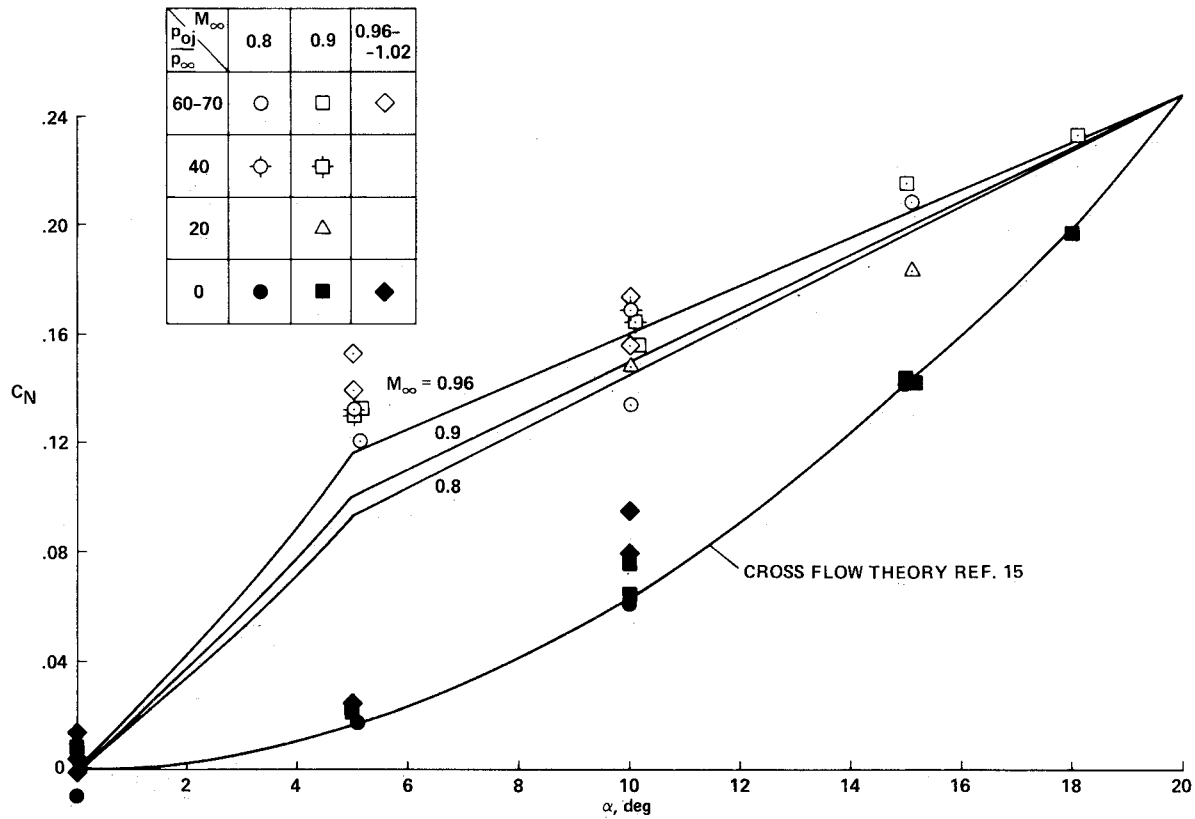

Fig. 10 Comparison of estimated normal force coefficient with experimental data.

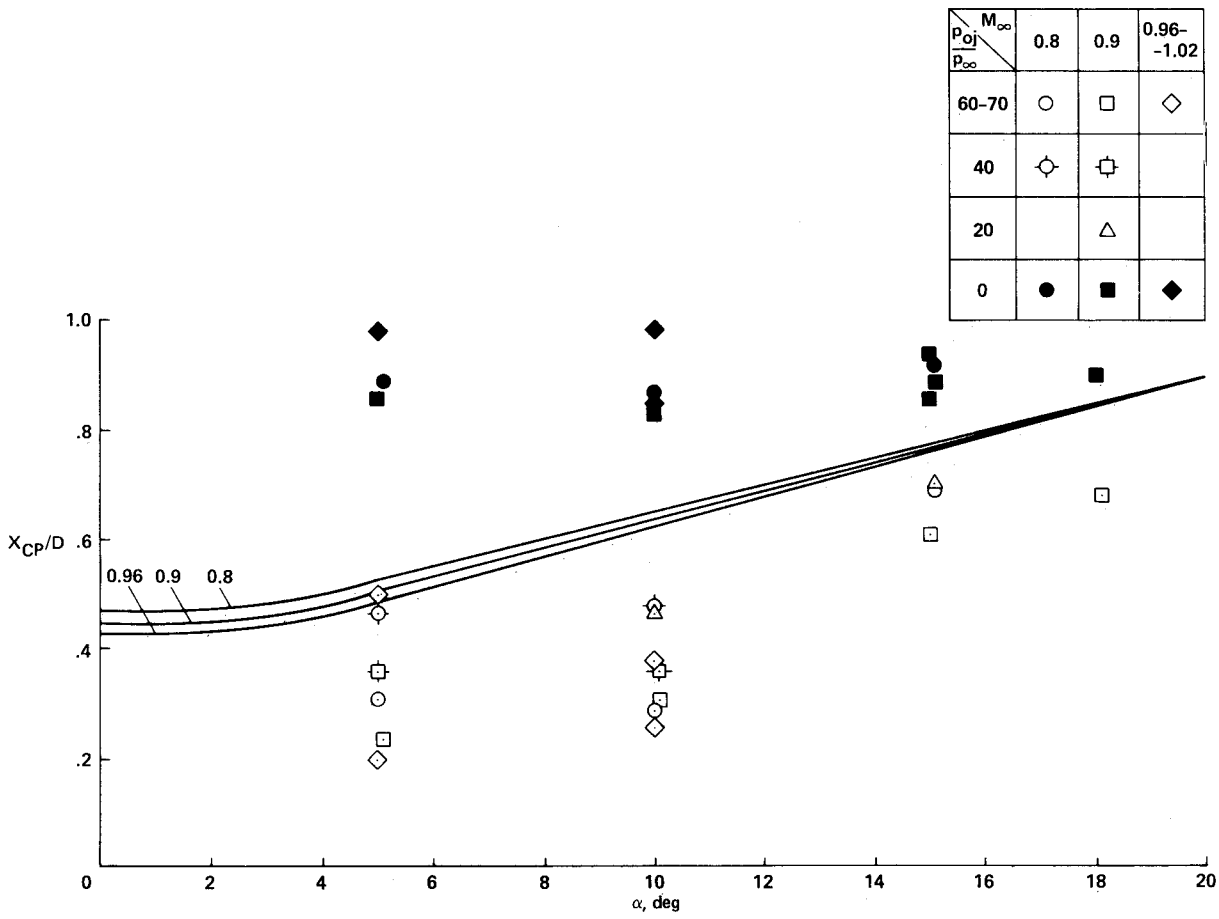

Fig. 11 Comparison of estimated center-of-pressure location with experimental data.

flare of 21 mm length and 2.73 deg semivertex angle at $M_\infty = 0.8$ and 0.9 and of 20 mm length and 3.58 deg semivertex angle at $M_\infty = 0.96$. These equivalent conical flares were used to compute the normal force coefficient and the center-of-pressure location for angles of attack between $\alpha = 0$ and 5 deg (Figs. 10 and 11), where most of the jet penetration effects are concentrated.[9] Since the jet-induced disturbance is distorted at higher angles of attack and does not remain axisymmetrical, such an approximation is valid at low angles of attack only. A linear variation between the flare-induced values and those of the cross-flow theory is, therefore, proposed for use in the angle-of-attack range between $\alpha = 5$ and 20 deg, where the jet-induced effects gradually decay and the crossflow mechanism becomes dominant. Also presented in Figs. 10 and 11 are the normal force coefficient and the location of the center-of-pressure variations with angle of attack as measured on the ogive cylinder model of Ref. 9 with several blowing pressure ratios. The equivalent conical flare results (solid lines) are in fair agreement with the experimental normal force coefficient data and display the correct trend when the Mach number is varied (Fig. 10). The agreement with the center-of-pressure data is only qualitative (Fig. 11). These data are strongly dependent on the blowing pressure ratio[9] (whereas the normal force is not) that has not been accounted for in the approximation of the equivalent conical flare.

The equivalent conical flare approximation cannot serve as a predictive method when experimental boundary-layer data have to be used. An approximation based on a generalized pressure distribution (e.g. Figs. 8b and 9b) would certainly be better. It would also account for the effects of the blowing pressure ratio. An even better predictive model should, probably, be an equivalent toroidal flare (or skirt) with its diameter equal to the proposed penetration height [Eq. (11)]. Such a model would more closely resemble the physical features of the flowfield and would account for all of the main flowfield parameters. Unfortunately, no experimental data for such a configuration were available to put this idea to the test.

Conclusions

A jet penetration height for transonic flow was derived both for a single jet perpendicular to a flat plate and for a large number of radial jets emitted from the circumference of an axisymmetrical body at zero angle of attack. Although not corresponding to any specific physical feature of the flowfield, the penetration height parameter was found to vary with Mach number and blowing pressure ratio changes in correspondence with the radius of curvature of the jets. It was also found to correlate the pressure distributions, obtained under different test conditions, on a single curve.

The solid-obstacle concept was extended to simple approximations of the variations in the normal force coefficient and center of pressure with the angle of attack, based on an equivalent cylinder flare model that could be used for engineering design purposes. Better approximations, based on a generalized, correlated pressure distribution or on the penetration height itself, were proposed, but were not verified.

References

[1]Spaid, F. W. and Zukoski, E. E., "A Study of the Interaction of Gaseous Jets from Transverse Slots with Supersonic External Flows," *AIAA Journal*, Vol. 6, Feb. 1968, pp. 205-212.

[2]Hsia, H.T.S., "Equivalence of Secondary Injection to a Blunt Body in Supersonic Flow," *AIAA Journal*, Vol. 4, Oct. 1966, pp. 1832-1834.

[3]Billig, F. S., Orth, R. C., and Laskey, M. A., "Unified Analysis of Gaseous Jets Penetration," *AIAA Journal*, Vol. 9, June 1971, pp. 1048-1058.

[4]Kallis, J. M., "Equivalent Solid Obstacle for Gas Injection into a Supersonic Stream," *AIAA Journal*, Vol. 10, Oct. 1972, pp. 1342-1344.

[5]Spaid, F. W., Zukoski, E.E., and Rosen, R., "A Study of Secondary Injection of Gases into a Supersonic Flow," NASA TR-32-834, 1966.

[6]Shapiro, A. H., *The Dynamics and Thermodynamics of Compressible Fluid Flow*, Vol. I, The Roland Press Co., New York, 1954, pp. 399-400.

[7]Spaid, F. W. and Cassel, L. A., "Aerodynamic Interference Induced by Reaction Controls," AGARD AG-173 (AD-775209), 1973.

[8]Heyser, A. and Maurer, F., "Experimentalle Untersuchungen an festen Spoilern und Strahlspoilern bei Machschen Zahlen von 0.6 bis 2.8," *Zeitschrift fuer Flugwissenschaften* Vol. 10, 1962, Heft 4/5.

[9]Seginer, A. and Manela, J., "Interaction of Multiple Supersonic Jets with a Transonic Flow Field," NASA TM 84369, May 1983 (also AIAA Paper 83-1680, July 1983).

[10]Spaid, F. W., "A Study of Secondary Injection of Gases into a Superonic Flow," Ph.D. Thesis, California Institute of Technology, Pasadena, 1964.

[11]Chrans, L. J. and Collins, D. J., "Stagnation Temperature and Molecular Weight Effects in Jet Penetration," *AIAA Journal*, Vol. 8, Feb. 1970, pp. 287-293.

[12]Hawk, H. E. and Amick, J. L., "Two-Dimensional Secondary Jet Interaction with a Supersonic Stream," *AIAA Journal*, Vol. 5, April 1967, pp. 650-655.

[13]Cohen, L. S., Coulter, L. J., and Egan, W. J. Jr., "Penetration and Mixing of Multiple Gas Jets Subjected to a Cross Flow," *AIAA Journal*, Vol. 9, April 1971, pp. 718-724.

[14]Manela, J., "The Influence of Jets, Injected Transversely into a Transonic Flow Near the Base of an Axisymmetric Configuration, on Flow Field, Lift and Stability Characteristics of the Body," M.Sc. Thesis, Technion—Israel Institute of Technology, Haifa, Nov. 1980.